LETTERS
PUBLISHED ONLINE: 24 JUNE 2012 | DOI: 10.1038/NCLIMATE1600
nature climate change

All flavours of El Niño have similar early subsurface origins

Nandini Ramesh[1]*† and Raghu Murtugudde[2]

The El Niño/Southern Oscillation phenomenon, characterized by anomalous sea surface temperatures and winds in the tropical Pacific, affects climate across the globe[1]. El Niños occur every 2–7 years, whereas the El Niño/Southern Oscillation itself varies on decadal timescales in frequency and amplitude, with a different spatial pattern of surface anomalies[2] each time the tropical Pacific undergoes a regime shift. Recent work has shown that Bjerknes feedback[3,4] (coupling of the atmosphere and the ocean through changes in equatorial winds driven by changes in sea surface temperature owing to suppression of equatorial upwelling in the east Pacific) is not necessary[5] for the development of an El Niño. Thus it is unclear what remains constant through regimes and is crucial for producing the anomalies recognized as El Niño. Here we show that the subsurface process of discharging warm waters always begins in the boreal summer/autumn of the year before the event (up to 18 months before the peak) independent of regimes, identifying the discharge process as fundamental to the El Niño onset. It is therefore imperative that models capture this process accurately to further our theoretical understanding, improve forecasts and predict how the El Niño/Southern Oscillation may respond to climate change.

A theoretical model that has been largely successful at explaining the El Niño/Southern Oscillation (ENSO) is the recharge oscillator[6,7], which views ENSO as a cycle in which the tropics are recharged with warm water[8] during the La Niña and neutral phases by the subtropical gyres and then discharge this water to the subtropics, producing warm anomalies in the form of an El Niño. The cycle's aperiodicity is attributed to weather noise, but whether ENSO is really cyclic or a series of events is debated[9,10]. A study using empirical orthogonal function analysis reveals a tilting of the equatorial thermocline[11] with two dominant spatial patterns: a meridional and a zonal pattern with the former leading the latter by approximately nine months. During the recharge phase, the thermocline deepens owing to the accumulation of warm water in the tropics. The onset of an El Niño is characterized by the flattening of the thermocline (the anomalous zonal tilt that brings about the discharge), but when and why this process begins remain unexplained.

ENSO also exhibits variability on decadal timescales[2] in terms of the amplitude, frequency and spatial distribution of surface anomalies. The changes in frequency and amplitude of ENSO do not seem to be significant if the changing background state in the tropical Pacific is accounted for[2], but the changes in surface expressions are not understood. The onset of the El Niños in the 1980s and 1990s began with warm sea surface temperature (SST) anomalies near the dateline that spread eastwards whereas earlier events began with anomalies off the west coast of South America and spread westwards[12]. El Niños followed this new pattern until the late 1990s (ref. 13), but another spatial pattern with warm anomalies concentrated in the central Pacific[14,15] rather than the eastern upwelling region, along with an amplitude and frequency change, has been dominant since 2000. These changes in spatial patterns raise an important question: if El Niño onset can occur without involving the eastern upwelling, is Bjerknes feedback essential to ENSO? An alternative mechanism, the thermally coupled Walker mode, has been proposed recently, which relies on latent heat fluxes rather than upwelling to provide atmosphere–ocean coupling[5], with the Bjerknes feedback serving only to strengthen events.

The apparent absence of any unchanging component in the development of ENSO events through regimes implies that we may not understand some fundamental aspects of the system. Each year, the Pacific experiences a seasonal cycle with a flattening of the zonal temperature gradient in boreal spring[16], but coupling occurs only in El Niño years. Some precursors that imply a persistence across the spring barrier have been identified[17–20] but the lack of coupling during most years implies that some aspect of the system is set before spring, preparing the Pacific for a growing mode leading to an El Niño later that year.

To identify the onset features that remain constant through regimes, we calculated separate composites for each of the three regimes (regime 1: 1958–1976; regime 2: 1977–2000; regime 3: 2001–2011) based on the observed regime shifts[21]. These composites were calculated by averaging various parameters for all El Niño events from June of the year before the event (referred to as year(−1)) to May of the year of the event (year(0)) where the peak of the event occurred during December of year(0) (see Methods).

Composite SSTs are warmer for El Niño years than those for all other years as early as June–August of year(−1) in the Niño-4 region. Figure 1 shows SST and wind-speed anomalies during June–November(−1) for each regime. Although the large-scale SST and wind patterns are not identical, a small positive SST anomaly can be seen in the far west Pacific (130°–160° E, 0°–15° S—indicated by the red box) in all regimes.

We found that surface heat fluxes over the west Pacific during June–August(−1) do not explain the appearance of this warm SST anomaly. Examining subsurface temperature anomalies (with respect to a climatology for the entire period) was more instructive. During this period, the west Pacific warm pool is anomalously warm beneath the surface in all three regimes (Fig. 2). The subsurface warm anomaly spreads across the Pacific, reaching the east coast by March–May of year(0). This subsurface anomaly seems to develop

[1]Divecha Centre for Climate Change, Indian Institute of Science, Bangalore 560012, India, [2]Earth System Science Interdisciplinary Center, University of Maryland, College Park, Maryland 20742, USA. †Present address: Climate Change Research Centre, University of New South Wales, Sydney 2052, Australia. *e-mail: nandini.ramesh@unsw.edu.au.

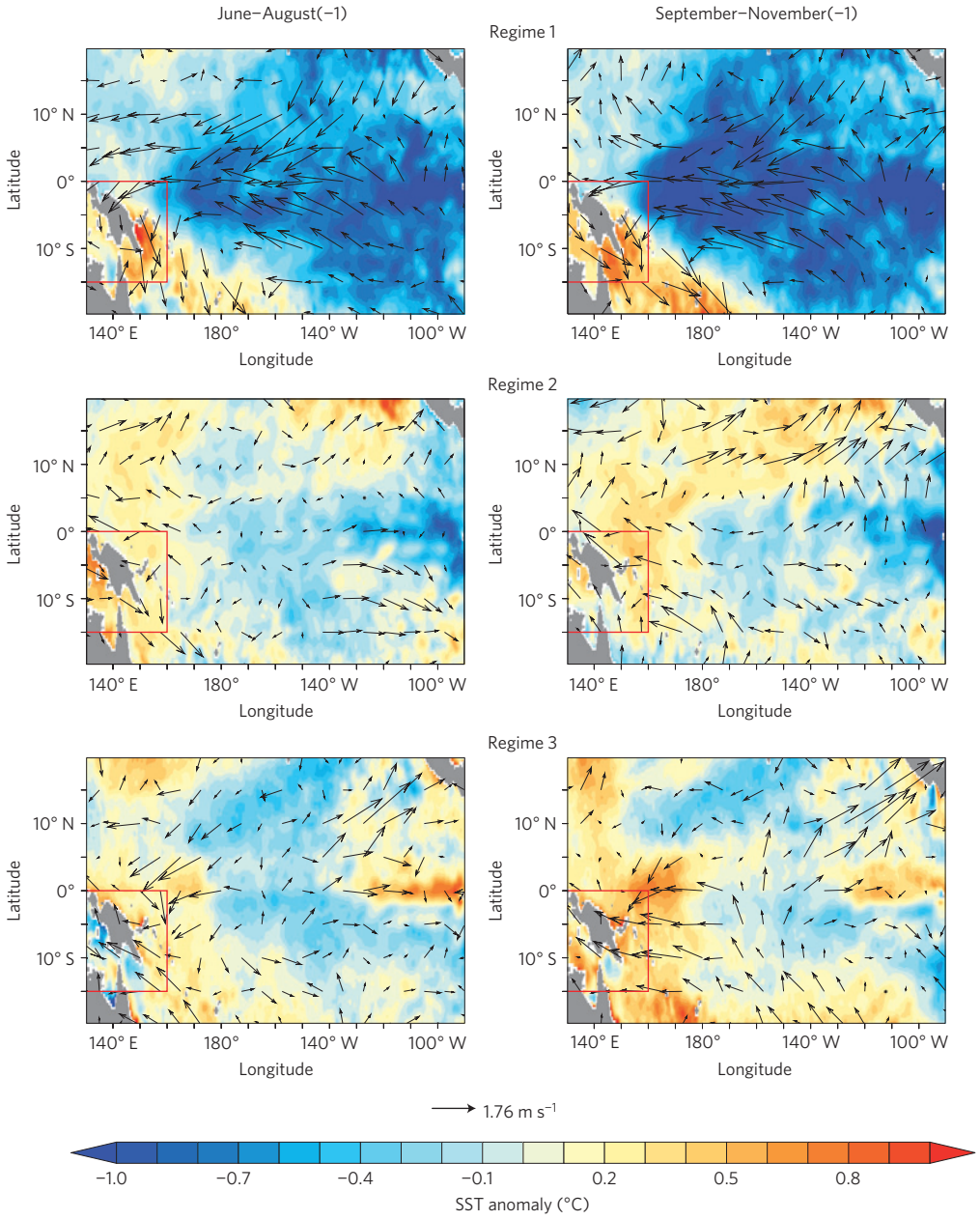

Figure 1 | SST anomalies for the El Niño composites calculated from SODA version 2.1.6 show that there is always a small warm anomaly in the west Pacific (130°–160° E, 0°–15° S, shown in red box) as early as June–August (−1). The wind anomalies (vectors) are from NCEP and National Center for Atmospheric Research Reanalysis, version 1.

differently in each regime. However, when we accounted for the changing background state in the Pacific[2] by calculating anomalies in each regime with respect to a separate climatology (computed as the mean seasonal cycle over only the duration of that regime) rather than a single long-term climatology, the process is seen to be nearly identical: the warm anomaly in the west spreads eastwards along the thermocline and reaches the surface in the east in March–May of year(0) as seen in Fig. 3. This west-to-east subsurface warming corresponds to the zonal flattening of the thermocline[12] and remains consistent through regimes. Despite the short duration of regime 3, the process is still unmistakable. This is remarkable because regime 3 included many central Pacific El Niños, which have a very different surface manifestation compared with canonical El Niños and have even been argued to have become the dominant flavour of El Niño with continued anthropogenic warming[22]. This implies that the onset of the discharge process has remained the same through all regimes, despite the dramatic differences in surface expressions, and must therefore be a process fundamental to the onset of El Niño and may remain so even in a warming world.

The scatter diagram of Fig. 4 shows the SST anomaly averaged over the area of warm SST anomaly in Fig. 1 (130°–160° E, 0°–15° S) in the far west Pacific and the thermocline-depth anomaly in the west Pacific (10° N–10° S, 150° E–150° W) in August for all years used in the study. The thermocline-depth anomaly represents the volume of accumulated warm tropical water beneath the surface (possibly the culmination of the meridional thermocline tilt), whereas the SST anomaly is the surface manifestation of the subsurface warm anomaly. All (−1) years (red crosses) fall into the top-right quadrant, with the exceptions of 1967, 1993 and 2005, all of which only ambiguously qualify as El Niño (−1) years[23] (see Methods). The SST anomaly may also be responsible for driving the wind anomalies seen in Fig. 1.

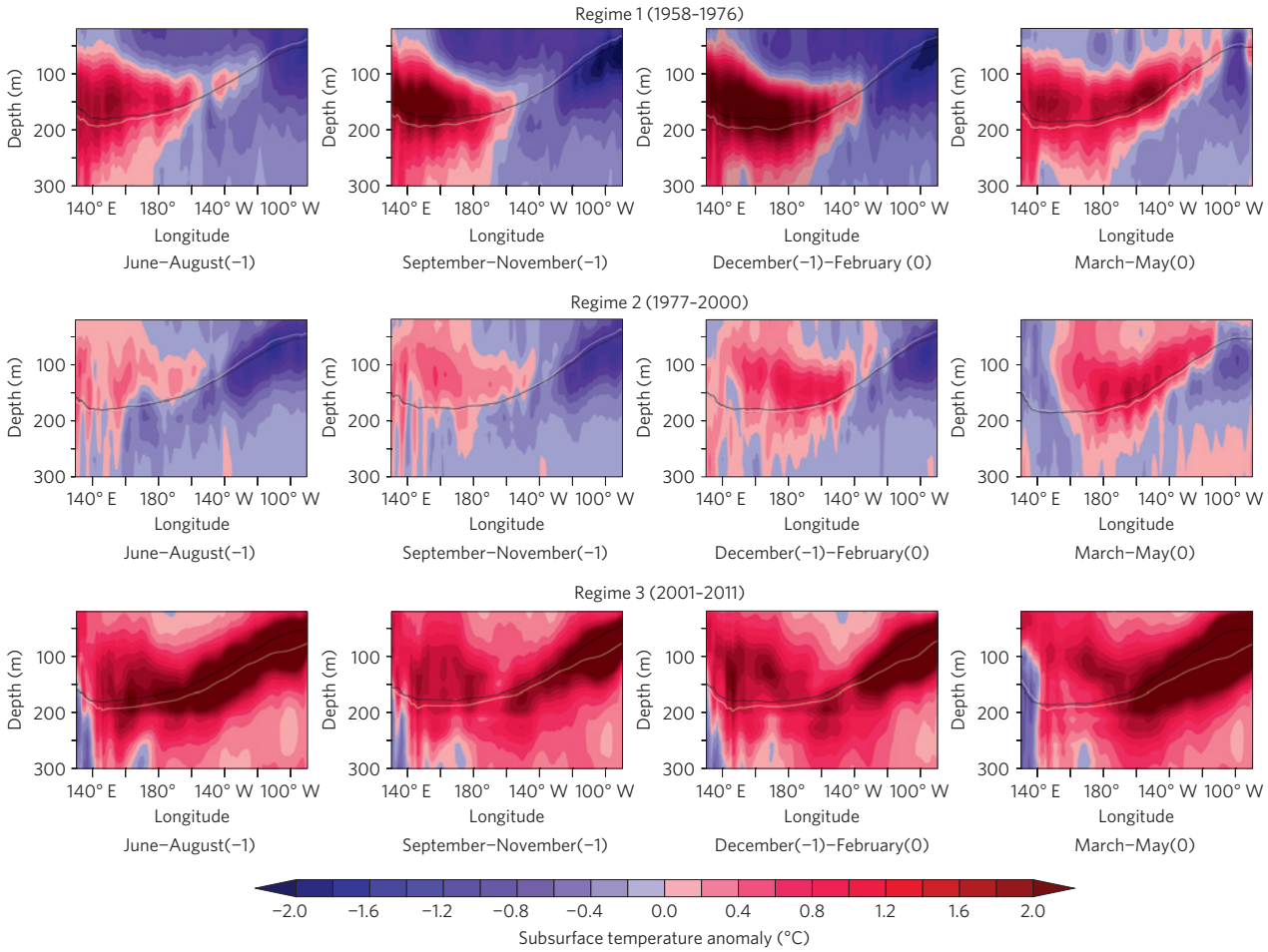

Figure 2 | Subsurface temperature anomalies of the El Niño composites from SODA version 2.1.6 calculated with respect to a long-term climatology show a warm SST anomaly in the west. The warm anomalies (averaged over 5° N–5° S) develop differently to reach the east coast by March–May(0). The black line represents the long-term climatological thermocline and the white line the thermocline for the composites.

The three years that are not El Niños but appear in this quadrant are 1974, 1978 and 1989. It was found that in these years, the discharge began in June–August but did not result in El Niños during the following year. Although warm anomalies did appear at the surface during the following year for both 1978 and 1989, these were not strong enough to qualify as El Niños. In the case of 1974, the discharge began, but the anomalies did not reach the surface in March–May(0). These aborted El Niños show that the initiation of the discharge is not a sufficient condition for the occurrence of an El Niño; it is possible that the discharge may be initiated by a trigger such as large-scale atmospheric variability.

The dramatic differences in SST and wind anomalies between El Niño events means that these may be a response to processes that are already underway, such as the subsurface discharge; in fact, the relationship between Bjerknes feedback and the spatial structure of surface anomalies is not evident in all El Niños, implying that this feedback cannot be fundamental to the onset of an El Niño. Although the Bjerknes feedback may occur in the early stages of a few events, there are many events where this is not the case, supporting this assertion (see Supplementary Information). The discharge manifested as warm subsurface anomalies spreading from west to east occurs nearly identically for all events at a deterministic stage in their life cycle, well in advance of the surface manifestations of El Niño. Therefore, the subsurface process can be considered a fundamental driver of ENSO onset whereas the surface manifestations follow later.

It is therefore critical that models focus on this subsurface process rather than the surface anomalies, which are merely a consequence of a more fundamental process at work, away from the eyes of satellites staring at the surface. The use of SSTs as an indicator is widespread and the existence of a myriad of SST-based indices[24] reflects the changing nature of surface anomalies; the resulting numerous lists of past El Niños[23] are both an indicator of and a cause for confusion. Although the SST and surface wind signatures are crucial for determining the global impacts of ENSO, focusing on the initiation of the discharge, which takes place well before any ENSO precursors known at present, will not only enhance our understanding of this phenomenon but should also lead to more reliable predictions with longer lead times. This fundamental aspect of the system may also provide a more robust framework for understanding the impact of global warming on ENSO, which has thus far remained highly uncertain[25].

It is important to note that although the focus of this work is the regime-independent subsurface process, there is, no doubt, a role played by the atmosphere in the onset of an El Niño event. Future work will detail the behaviour of the atmosphere during the early stages of ENSO onset. Further studies will also examine the triggers for the discharge process, attempt to identify a sufficient condition to produce an El Niño and trace the development of El Niño events beyond August(−1) including the role of Bjerknes feedback and the potential impact of anthropogenic warming on these processes. The totality of natural and anthropogenic ENSO changes can be deciphered only

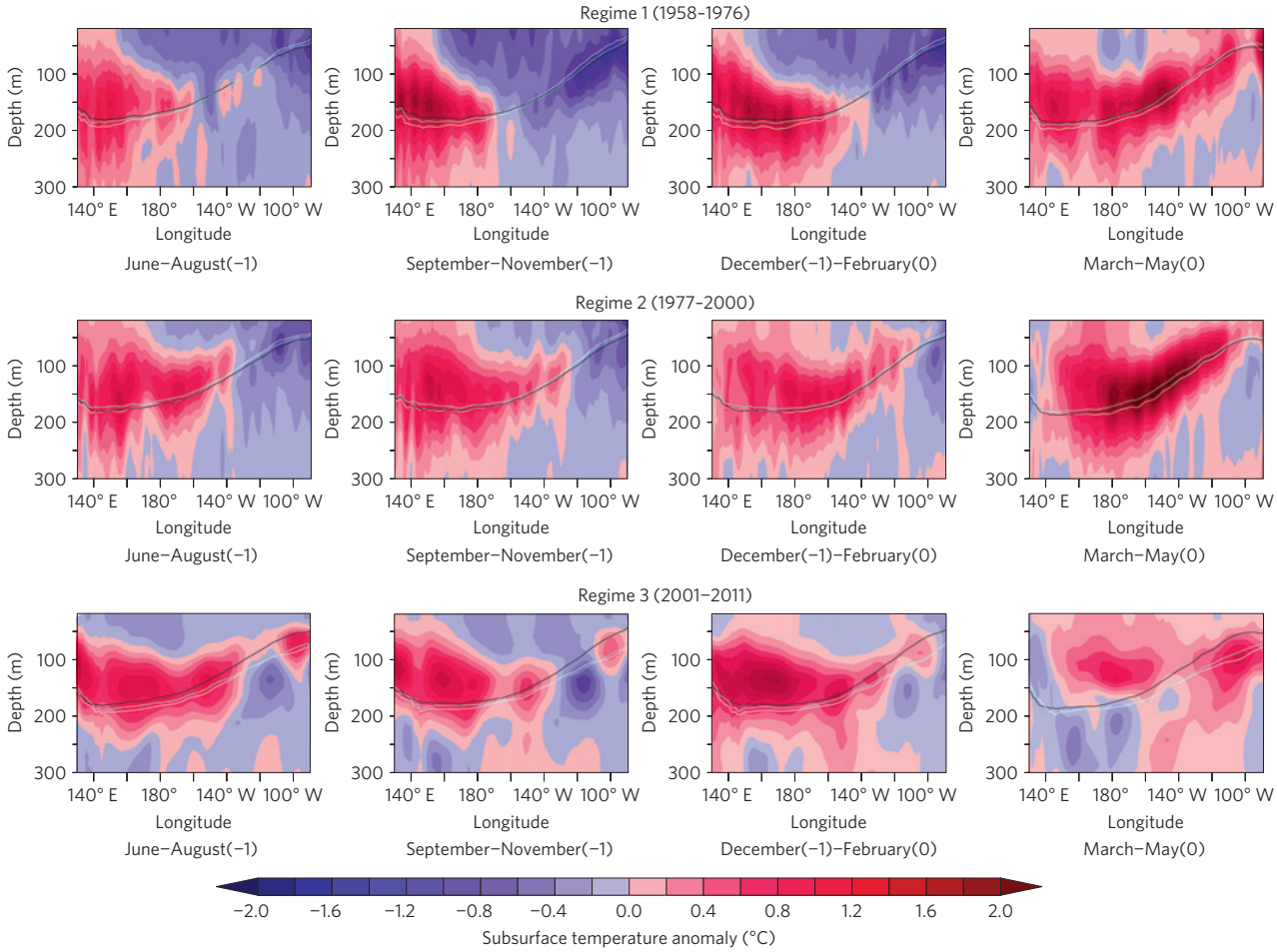

Figure 3 | Subsurface temperature anomalies (averaged over 5° N–5° S) for the El Niño composites calculated with respect to a separate climatology for each period show that the warm anomaly spreads from the west in June–August (−1) along the thermocline to reach the east in March–May(0) in all three regimes. The black and white lines are the same as those in Fig. 2, whereas the blue line represents the thermocline from the regime-specific climatology.

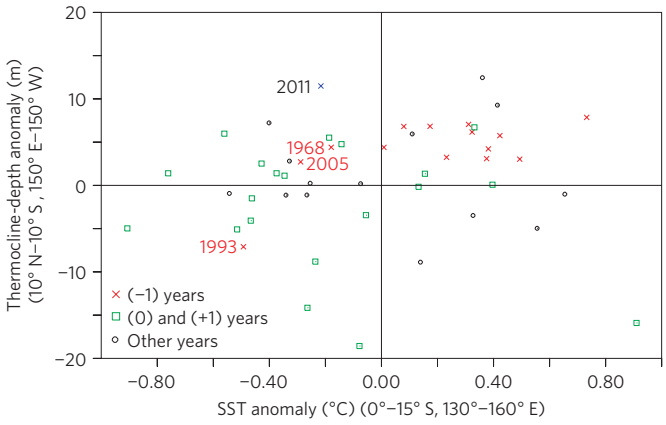

Figure 4 | Plotting August averages of each year on a scatter diagram shows that all El Niño(−1) years (red crosses) fall into the top-right quadrant, meaning they all have positive values of thermocline-depth anomaly in 10° N–10° S, 150° E–150° W and SST anomaly in 130°–160° E, 0°–15° S. There is ambiguity over whether 1968, 1993 and 2005 were El Niño (−1) years and these fall outside of this quadrant. Three non-El Niño years (black symbols) also fall into the top-right quadrant and are aborted El Niños. The green squares represent El Niño(0) and (+1) years. 2011 is marked with a blue cross.

by filling these gaps in our understanding of this phenomenon with a global reach.

Methods

The calculation of El Niño composites for each regime was carried out by computing the average value over all El Niño years in that regime for each month of the period from June(−1) to May(0). The El Niño years used to calculate the composites were chosen based on the Climate Prediction Center's Niño 3.4 criteria, according to which a year qualifies as an El Niño year if the three-month running mean of the SST anomaly in the Niño 3.4 region (120°–170° W, 5° N–5° S) remains above or equal to 0.5 °C for five consecutive months. The El Niño years used in this study (listed as year 0 of the composite) based on these criteria are: Regime 1: 1963, 1965, 1972, 1976; Regime 2: 1982, 1986, 1991, 1997; Regime 3: 2002, 2004, 2009. Although 1968–1969, 1994 and 2006 also qualify as El Niño years according to the Climate Prediction Center's criteria, there is some ambiguity as to whether these were truly El Niño events[23]. In 1968, the warming in the Niño 3.4 region was weak and was not accompanied by warming in any of the other Niño index regions (all other years used showed warming in at least one of the other index regions). The same was true of 1969, which may have been a continuation of the weak warming in 1968. 1994 was not considered because it was a continuation of warming that had begun in 1990 (ref. 26) and therefore would not show the onset features of interest here. The event of 2006 cannot qualify as an El Niño event according to several measures; those measures that do consider it an El Niño event disagree as to whether it was a central Pacific or canonical event.

Where inferences were made based on a feature observed in a composite, each of the years used in the calculation of the composite was examined individually to ensure that the feature was present.

SST data from National Oceanic and Atmospheric Administration Optimum Interpolation (0.25° daily) blended with Advanced Very High Resolution

Radiometer SST version 2 (1981–2009), Simple Ocean Data Assimilation (SODA) version 2.1.6 (1958–2008, five daily, $1^\circ \times 1^\circ$) and Hadley SST analyses (1870–2008, monthly, $1^\circ \times 1^\circ$) were compared to confirm the existence of the signal in the west Pacific in June–August(−1). Wind-stress data were taken from National Center for Environmental Prediction (NCEP) and National Center for Atmospheric Research Reanalysis, version 1 (1948–2008, monthly, $2^\circ \times 2^\circ$). Surface fluxes were also taken from this data set. Subsurface temperatures were from SODA version 2.1.6 (1958–2008, monthly, $1^\circ \times 1^\circ$). For the third regime, the SSTs used were from the Global High-Resolution SST data set (1981–present, daily, $0.25^\circ \times 0.25^\circ$) and the subsurface temperatures from the NCEP Global Ocean Data Assimilation System data set (1980–present, monthly, $1/3^\circ \times 1/3^\circ$) averaged to the same grid as the SODA data.

All calculations, analyses and figure production in this work were carried out using the Ferret program, a product of National Oceanic and Atmospheric Administration's Pacific Marine Environmental Laboratory.

Received 22 August 2011; accepted 23 May 2012; published online 24 June 2012

References

1. Alexander, M. *et al.* The atmospheric bridge: The influence of ENSO teleconnections on air–sea interaction over the global oceans. *J. Clim.* **15,** 2205–2228 (2002).
2. Fedorov, A. V. & Philander, S. G. Is El Niño changing? *Science* **288,** 1997–2002 (2000).
3. Bjerknes, J. Atmospheric teleconnections from the equatorial Pacific. *Mon. Weath. Rev.* **97,** 163–172 (1969).
4. Bjerknes, J. A possible response of the atmospheric Hadley circulation to equatorial anomalies of ocean temperature. *Tellus* **18,** 820–829 (1966).
5. Clement, A. C., DiNezio, P. & Deser, C. Rethinking the ocean's role in the Southern Oscillation. *J. Clim.* **24,** 4056–4072 (2011).
6. Jin, F-F. An equatorial ocean recharge paradigm for ENSO. Part I: Conceptual model. *J. Atmos. Sci.* **54,** 811–829 (1997).
7. Jin, F-F. An equatorial ocean recharge paradigm for ENSO. Part II: A stripped-down coupled model. *J. Atmos. Sci.* **54,** 830–847 (1997).
8. Wyrtki, K. Water displacements in the Pacific and the genesis of El Niño cycles. *J. Geophys. Res.* **90,** 7129–7132 (1985).
9. Philander, S. G. & Fedorov, A. V. Is El Niño sporadic or cyclic? *Annu. Rev. Earth Planet. Sci.* **31,** 579–594 (2003).
10. Kessler, W. Is ENSO a cycle or a series of events? *Geophys. Res. Lett.* **29,** 2125–2128 (2002).
11. Meinen, C. S. & McPhaden, M. J. Observations of warm water volume changes in the equatorial pacific and their relationship to El Niño and La Niña. *J. Clim.* **13,** 3551–3559 (2001).
12. Rasmussen, E. M. & Carpenter, T. H. Variations in sea surface temperature and surface wind fields associated with the Southern Oscillation/El Niño. *Mon. Weath. Rev.* **110,** 354–384 (1982).
13. Wang, B. & An, S. I. A mechanism for decadal changes of ENSO behavior: Roles of background wind changes. *Clim. Dynam.* **18,** 475–486 (2002).
14. Kao, H-Y. & Yu, J-Y. Contrasting Eastern-Pacific and Central-Pacific types of ENSO. *J. Clim.* **22,** 615–632 (2009).
15. Lee, T. & McPhaden, M. J. Increasing intensity of El Niño in the central-equatorial Pacific. *Geophys. Res. Lett.* **37,** L14603 (2010).
16. Webster, P. J. The annual cycle and the predictability of the tropical coupled ocean–atmosphere system. *Meteorol. Atmos. Phys.* **56,** 33–55 (1994).
17. Chang, P. *et al.* Pacific meridional mode and El Niño—Southern Oscillation. *Geophys. Res. Lett.* **34,** L16608 (2007).
18. Vimont, D. J., Wallace, J. M. & Battisti, D. S. The seasonal footprinting mechanism in the Pacific: Implications for ENSO. *J. Clim.* **16,** 2668–2675 (2003).
19. Lengaigne, M. *et al.* Triggering of El Niño by westerly wind events in a coupled general circulation model. *Clim. Dynam.* **23,** 601–620 (2004).
20. Torrence, C. & Webster, P. J. The annual cycle of persistence in the El Niño-Southern Oscillation. *Q. J. R. Meteorol. Soc.* **125,** 1985–2004 (1994).
21. Swanson, K. L. & Tsonis, A. A. Has the climate recently shifted? *Geophys. Res. Lett.* **36,** L06711 (2009).
22. Yeh, S. W. *et al.* El Niño in a changing climate. *Nature* **461,** 511–514 (2009).
23. Singh, A., Delcroix, T. & Cravatte, S. Contrasting the flavours of El Niño-Southern Oscillation using sea surface salinity observations. *J. Geophys. Res.* **116,** C06016 (2011).
24. Trenberth, K. E. The definition of El Niño. *Bull. Am. Meteorol. Soc.* **78,** 2771–2777 (1997).
25. Collins, M. *et al.* The impact of global warming on the tropical Pacific Ocean and El Niño. *Nature Geosci.* **3,** 391–397 (2010).
26. Trenberth, K. E. & Hoar, T. J. The 1990–1995 El Niño-Southern Oscillation event: Longest on record. *Geophys. Res. Lett.* **23,** 57–60 (1996).

Acknowledgements

This work was carried out at the Divecha Centre for Climate Change, Indian Institute of Science, Bangalore—560012, India, enabled by grants from the same. The authors would like to thank J. Beauchamp for providing the SODA, Global Ocean Data Assimilation System and Global High-Resolution SST data. N.R. would like to thank S. R. Parampil for assistance with the Ferret software.

Author contributions

Analysis of the data, production of the figures and writing of the final manuscript was carried out by N.R. The project was supervised and directed by R.M. who interpreted results and also edited the final manuscript.

Additional information

The authors declare no competing financial interests. Supplementary information accompanies this paper on www.nature.com/natureclimatechange. Reprints and permissions information is available online at www.nature.com/reprints. Correspondence and requests for materials should be addressed to N.R.